# Mapping of the RNA recognition site of Escherichia coli ribosomal protein S7

F. Robert, M. Gagnon, D. Sans, S. Michnick and L. Brakier-Gingras

*RNA* 2000 6: 1649-1659

*RNA* (2000), *6*:1649–1659. Cambridge University Press. Printed in the USA.


# Mapping of the RNA recognition site of *Escherichia coli* ribosomal protein S7

**FRANCIS ROBERT, MATTHIEU GAGNON, DIMITRI SANS, STEPHEN MICHNICK, and LÉA BRAKIER-GINGRAS**

Département de Biochimie, Université de Montréal, Montréal, Québec H3C 3J7, Canada

## ABSTRACT

**Bacterial ribosomal protein S7 initiates the folding of the 3′ major domain of 16S ribosomal RNA by binding to its lower half. The X-ray structure of protein S7 from thermophilic bacteria was recently solved and found to be a modular structure, consisting of an $\alpha$-helical domain with a $\beta$-ribbon extension. To gain further insights into its interaction with rRNA, we cloned the S7 gene from *Escherichia coli* K12 into a pET expression vector and introduced 4 deletions and 12 amino acid substitutions in the protein sequence. The binding of each mutant to the lower half of the 3′ major domain of 16S rRNA was assessed by filtration on nitrocellulose membranes. Deletion of the N-terminal 17 residues or deletion of the $\beta$ hairpins (residues 72–89) severely decreased S7 affinity for the rRNA. Truncation of the C-terminal portion (residues 138–178), which includes part of the terminal $\alpha$-helix, significantly affected S7 binding, whereas a shorter truncation (residues 148–178) only marginally influenced its binding. Severe effects were also observed with several strategic point mutations located throughout the protein, including Q8A and F17G in the N-terminal region, and K35Q, G54S, K113Q, and M115G in loops connecting the $\alpha$-helices. Our results are consistent with the occurrence of several sites of contact between S7 and the 16S rRNA, in line with its role in the folding of the 3′ major domain.**

**Keywords: 16S rRNA; ribosomal protein S7; RNA–protein interactions**

## INTRODUCTION

Bacterial ribosomal protein S7 is one of the primary proteins that, along with S4, initiates the higher-order folding of 16S ribosomal RNA and therefore the assembly of the 30S ribosomal subunit (Nowotny & Nierhaus, 1988). Besides its role in the ribosome, S7 also acts as a translational repressor for its own mRNA, the *str* operon mRNA, which codes for ribosomal proteins S7 and S12 and elongation factors EF-Tu and EF-G (Saito & Nomura, 1994; Saito et al., 1994). S7 binds to the lower half of the 3′ major domain of 16S rRNA (Fig. 1A), as demonstrated by crosslinking studies (Urlaub et al., 1995, 1997; Mueller & Brimacombe, 1997) as well as by protection against attack with base-specific chemical reagents or hydroxyl radicals (Powers et al., 1988; Powers & Noller, 1995). We previously showed that the S7-binding site on 16S rRNA could be delimited to a fragment of about 100 nt in the lower half of the 3′ major domain of 16S rRNA (Fig. 1B), containing helix 29, a portion of helix 42, helix 43, and two large internal loops, A and B, connecting helix 29 to helix 42 and to helix 43, respectively. This study also suggested that helix 29, the beginning of helix 43, and both loops A and B interacted with protein S7 (Dragon & Brakier-Gingras, 1993; Dragon et al., 1994).

The structure of protein S7 from two thermophilic bacteria, *Bacillus stearothermophilus* and *Thermus thermophilus*, has been solved independently by Hosaka et al. (1997) and Wimberly et al. (1997), respectively. The two structures are identical, suggesting that *Escherichia coli* S7 could also adopt the same structure. This suggestion is supported by the fact that *T. thermophilus* S7 can be assembled in vivo into the ribosome of *E. coli* (Karginov et al., 1995) and binds in vitro to an *E. coli* fragment containing the S7 binding site, with an affinity comparable to that of *E. coli* S7 (Spiridonova et al., 1998). The structure of protein S7 consists of a six $\alpha$-helix bundle with a $\beta$ hairpin between helices 3 and 4 (Fig. 2). The N- and C-terminal portions are disordered and exposed. RNA-binding regions could

Reprint requests to: Léa Brakier-Gingras, Département de Biochimie, Université de Montréal, Montréal, Québec H3C 3J7, Canada; e-mail: gingras@bcm.umontreal.ca.

*Abbreviations:* CD: circular dichroism; IPTG: isopropyl-$\beta$-D-thiogalactopyranoside; Ni-NTA: nickel-nitriloacetic acid; PCR: polymerase chain reaction; PMSF: phenylmethylsulfonyl fluoride; SDS-PAGE:, sodium dodecyl sulfate polyacrylamide gel electrophoresis. Abbreviations for the amino acid residues are as follows: A for alanine, F for phenyalanine, G for glycine, K for lysine, M for methionine, Q for glutamine, R for arginine, S for serine, Y for tyrosine.

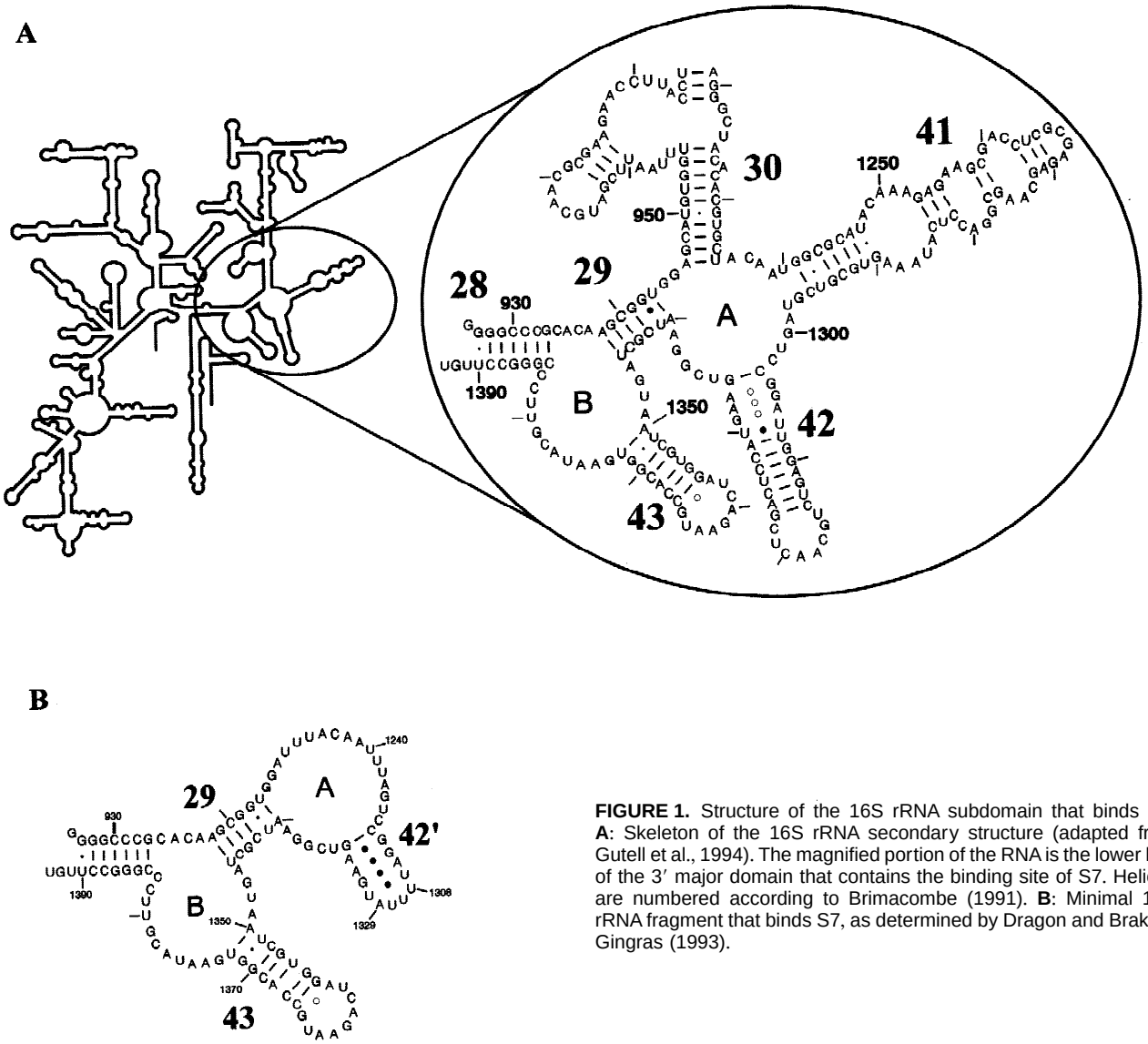


**FIGURE 1.** Structure of the 16S rRNA subdomain that binds S7. **A**: Skeleton of the 16S rRNA secondary structure (adapted from Gutell et al., 1994). The magnified portion of the RNA is the lower half of the 3′ major domain that contains the binding site of S7. Helices are numbered according to Brimacombe (1991). **B**: Minimal 16S rRNA fragment that binds S7, as determined by Dragon and Brakier-Gingras (1993).

be predicted from the analysis of S7 structure: first, a large concave surface, rich in basic and hydrophobic residues, involving the $\beta$ hairpin and portions of helices 4 and 6 plus the flexible N and C termini that can extend this surface; second, loop 2, bridging helices 1 and 2, and the proximal loop 5, which connects helices 4 and 5. These predictions are supported by crosslinking studies (Fig. 2) of the bacterial protein S7 to 16S rRNA within the 30S subunit, showing that both K8 and K75, located in the concave domain of the protein, can be crosslinked to nt 1378 in 16S rRNA, whereas M115, in loop 5, can be crosslinked to nt 1240 (Urlaub et al., 1995, 1997).

S7 is located in the head of the 30S subunit at the subunit interface (Capel et al., 1987; Mueller & Brimacombe, 1997; Cate et al., 1999; Clemons et al., 1999; Tocilj et al., 1999), close to the decoding region (Muralikrishna & Cooperman, 1994) and the 530 loop of 16S rRNA (Alexander et al., 1994). S7 was also crosslinked to the anticodon loop of tRNA at the A, P, and E sites (Sylvers et al., 1992; Döring et al., 1994; Rosen & Zimmermann, 1997), and to the mRNA upstream from the decoding site (Dontsova et al., 1992; Greuer et al., 1999). It is involved in the binding of tetracycline, an antibiotic that binds to the A site (Buck & Cooperman, 1990) and has been shown to crosslink to puromycin, another protein synthesis inhibitor that interacts with the A site (Bischof et al., 1994).

In this study, we have introduced various deletion and substitution mutations in several portions of *E. coli* S7 to gain further insights into its interaction with 16S rRNA.

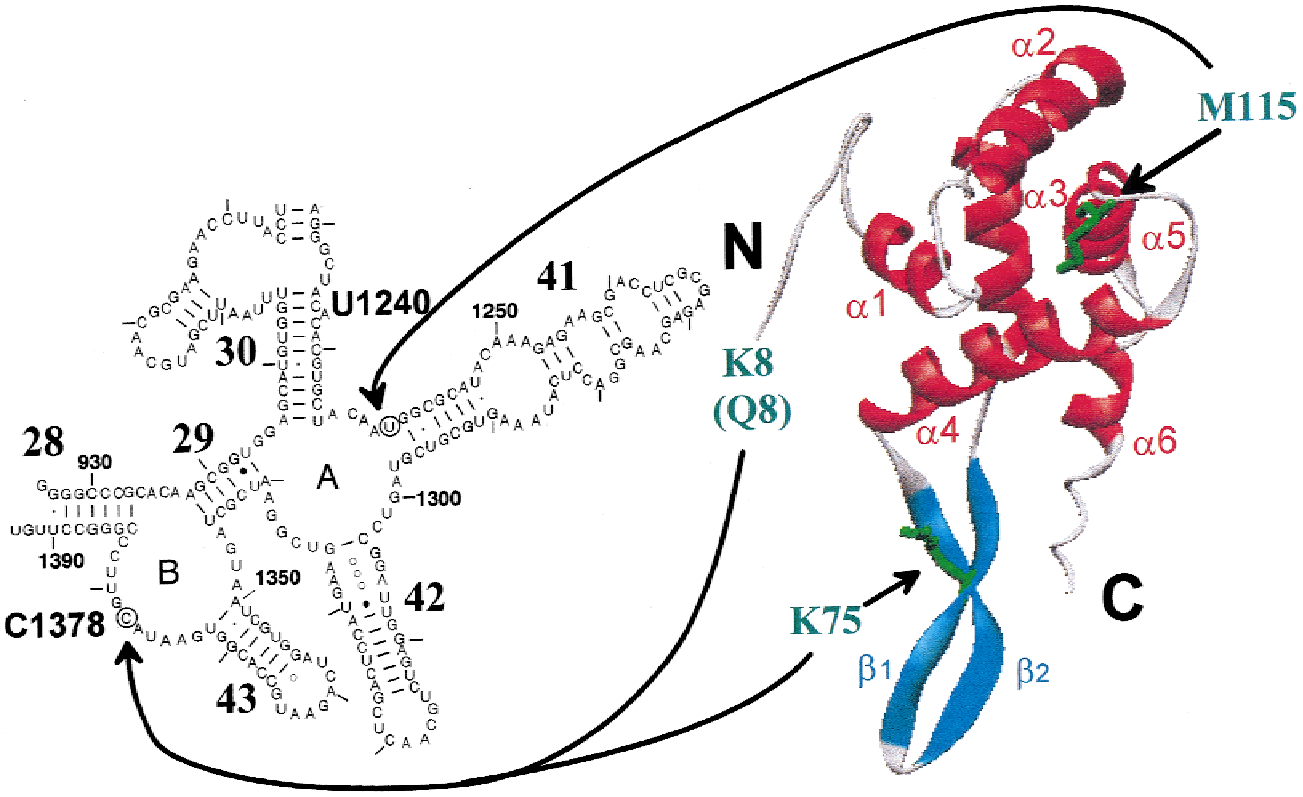


**FIGURE 2.** Crosslink sites between protein S7 and 16S rRNA within the 30S subunit. Left: secondary structure of the RNA-binding site of S7 showing bases U1240 and C1378 (circled) that have been crosslinked to the protein. Right: crystallographic structure of *B. stearothermophilus* S7 adapted from Hosaka et al. (1997) showing residues crosslinked to the rRNA at positions 8, 75, and 115. The crosslink at position 8 was found with *B. stearothermophilus* S7 (where it is K, whereas it is Q in *E. coli* S7), the crosslink of K75 was found with *E. coli* S7, and that of M115 with both *E. coli* and *B. stearothermophilus* S7. The concave surface encompassing the $\beta$ hairpin and parts of helices 4 and 6, to which we refer in the text, faces the reader. The S7 image was produced using Weblab ViewerPro software (Molecular Simulation Inc.).

## RESULTS

### Binding of *E. coli* S7 protein to 16S ribosomal RNA

The S7 gene from *E. coli* K12A19 chromosomal DNA was first cloned by PCR into plasmid pET-21a(+) under control of a T7 promoter (Studier et al., 1990) and its expression was induced with IPTG in *E. coli* BL21(DE3). A histidine tag was added to the N-terminal portion of the protein, and the protein was purified by chromatography on a Ni-NTA column under native conditions. The purity of the protein and that of its mutant derivatives described below was superior to 98%, as assessed by SDS-PAGE (data not shown). The affinity of the protein for its RNA-binding domain, in the lower half of the 3′ major domain of 16S rRNA, was measured by filtration on nitrocellulose membranes. For these assays, we used an RNA fragment generated by in vitro transcription that corresponds to the lower half of the 3′ major domain. With the nitrocellulose filtration binding assay, 100% of the RNA transcript is never retained on the filter (see Gregory et al., 1988). In the present study, saturation with wild-type S7 was observed when about 40% of the RNA transcript was bound to the filter (Fig. 4). The apparent association constant ($K'_a$) between S7 and the rRNA fragment was determined from the amount of protein required to half-saturate the RNA. It was found to be 5.3 $\mu M^{-1}$ when binding assays were performed in a high-ionic-strength buffer (20 mM $MgCl_2$, 300 mM KCl), which is classically used for 30S subunit assembly in vitro (Table 1). This value is about threefold higher than the value we observed previously with S7 purified without a histidine tag under denaturing conditions (Dragon & Brakier-Gingras, 1993). This increase in the affinity of S7 for the rRNA does not appear to result from the presence of the histidine tag. Indeed, as shown below, some mutant derivatives of S7 bind very poorly to the rRNA although they have this histidine tag. It is more likely that this increase results from the fact that S7 was purified under native conditions in the present study (see also Spiridonova et al., 1998). When binding assays were performed in a moderate-ionic-strength buffer (2 mM $MgCl_2$, 175 mM KCl), under conditions that are closer to physiological salt conditions (Kao-Huang et al., 1977), the associa-

**TABLE 1**. Affinity for 16S rRNA of wild-type S7 and deletion mutants.

| Mutant | High ionic strength[a] | | Moderate ionic strength[b] | |
|---|---|---|---|---|
| | $K'_a$[c] ($\mu M^{-1}$) | Relative affinity | $K'_a$[c] ($\mu M^{-1}$) | Relative affinity |
| Wild-type S7 | 5.3 ± 0.5 | 1.00 | 30.5 ± 3.8 | 1.00 |
| Δ1–17 | n.d.[d] | — | 2.0 ± 0.4 | 0.07 |
| Δ72–89 | 1.8 ± 0.3 | 0.34 | 6.1 ± 1.0 | 0.20 |
| Δ138–178 | 3.1 ± 0.5 | 0.58 | 9.8 ± 1.8 | 0.32 |
| Δ148–178 | 5.6 ± 0.7 | 1.06 | 16.9 ± 2.3 | 0.55 |

[a]High-ionic-strength buffer is 20 mM $MgCl_2$, 300 mM KCl.
[b]Moderate-ionic-strength buffer is 2 mM $MgCl_2$, 175 mM KCl.
[c]$K'_a$ values are means and standard deviation of at least four independent experiments.
[d]n.d.: not detectable.

tion constant was increased about sixfold compared to its value in the high-ionic-strength buffer (Table 1). This likely reflects the involvement of electrostatic interactions between S7 and the rRNA, which are less efficient in a high-ionic-strength buffer (Draper, 1999).

### Identification of the regions of S7 involved in its binding to 16S rRNA using deletion mutations

Various deletion mutants were first investigated to dissect out the regions of S7 involved in rRNA binding (Fig. 3). The unstructured N-terminal portion (residues 1–17)[1] preceding helix 1, and the C-terminal portion (residues 138–178), including the unstructured C-terminal region plus a part of helix 6, were deleted independently. A shorter C-terminal truncation (Δ148–178), where only the unstructured C-terminal region was eliminated, was investigated as well. The β hairpin (residues 72–89), located between helices 3 and 4, was also deleted and replaced with a short flexible loop, RRGGGGS, recreating the charge environment normally found in this region of the protein. The CD spectra confirmed that protein S7 has a high content of secondary structure as shown in earlier CD studies (Dijk et al., 1986) and did not reveal any significant difference between wild-type S7 and the four deletion mutants, suggesting that the secondary structure of S7 and that of its mutants are very similar (data not shown). This indicates that the truncated proteins did not suffer major structural perturbations except for the deletion. However, it cannot be excluded that minor changes could have occurred in the tertiary folding of some mutants.

Affinities for the lower half of the 3′ major domain of 16S rRNA were measured in the high-ionic-strength and the moderate-ionic-strength buffers (Fig. 4 and Table 1). Our results show that each deletion interfered with S7 binding to the 16S rRNA fragment, the effect being greatest for the deletion in the N-terminal portion. Indeed, with this mutant, there was no detectable binding in the high-ionic-strength buffer, whereas a very low level of binding could be detected in the moderate-ionic-strength buffer, with an association constant that was reduced more than 10-fold relative to wild-type S7. Deletion of the β hairpin also interfered strongly with the binding, the association constant being reduced about three- and fivefold in the high- and moderate-ionic-strength buffer, respectively. The large C-terminal deletion (Δ138–178) reduced the affinity two- and threefold in the high- and moderate-ionic-strength buffer, respectively. The short C-terminal deletion (Δ148–178) had no effect in the high-ionic-strength buffer and caused only a weak effect in the moderate-ionic-strength buffer. Altogether, these results suggest that the N-terminal portion of the protein as well as the β hairpin play a major role in S7 binding to the 16S rRNA. Helix 6 is also involved in S7 binding although to a lesser extent. The effects of the deletion of the β hairpin and of the C-terminal region were increased in the moderate-ionic-strength buffer, probably reflecting the loss of electrostatic interactions between S7 and the 16S rRNA. The N-terminal portion of S7 contains several charged residues that likely interact with 16S rRNA, but the low binding capacity of the N-terminal deletion mutant makes it difficult to assess the importance of electrostatic interactions in the N-terminal region.

### Identification of amino acid residues of S7 involved in its binding to 16S rRNA using point mutations

To define which amino acid residues of S7 are involved in binding to rRNA, we mutated the protein at 12 different positions, not only in the regions that we previously deleted but also in other parts of the protein likely to be involved in the protein–RNA interactions (Fig. 3). The residues mutated were chosen according to their conservation and exposure to solvent determined from the S7 crystal structure (Hosaka et al., 1997; Wimberly et al., 1997). Each mutant was expressed in *E. coli* and purified as described above. Point mutations were introduced in the N-terminal portion (R3Q, Q8A, and F17G), in the β hairpin (Y84A), and in helix 6, preceding the C-terminal unstructured portion (K136Q, R142Q, and M143A). Mutations were also introduced in loop 2 (K34Q and K35Q), in loop 3 (G54S), and in loop 5 (K113Q and M115G). The mutations of K or R to Q conserve the capacity of the residues to interact with rRNA through hydrogen bonding but not through a salt bridge. Again, the CD spectra of all the point mutants were very similar to that of wild-type S7, which suggests that the secondary structure of S7 was not al-

[1]Numbering is that of Reinbolt et al. (1978) for *E. coli* S7, except that it was corrected for the omission of amino acid R91 in the original report, as later shown by sequencing of the gene (Johanson & Hughes, 1992).

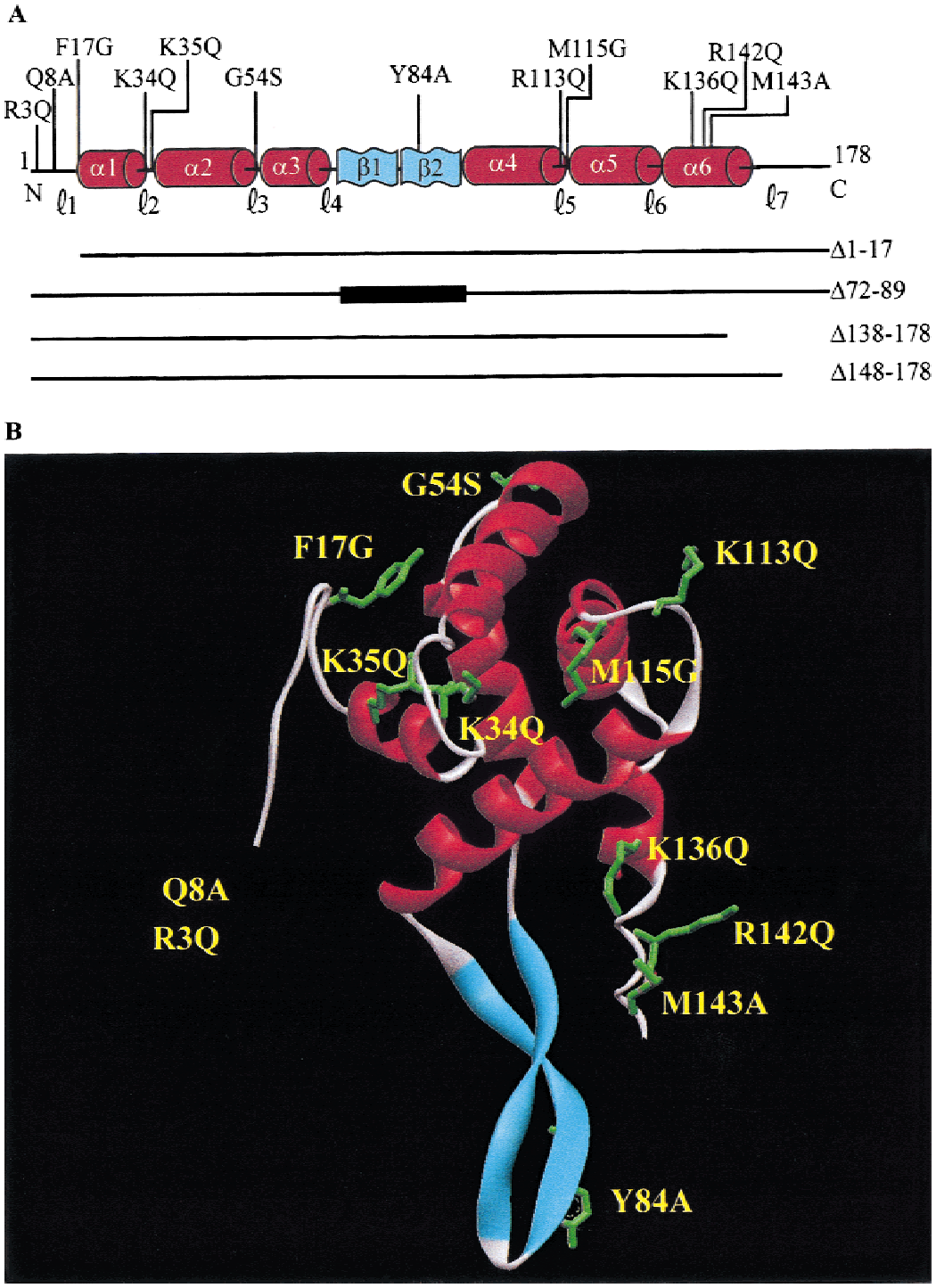


**FIGURE 3.** Mutations in *E. coli* protein S7. **A**: Schematic representation of the different S7 mutations that were investigated in this study. $\ell 1$ to $\ell 7$ correspond to loop 1 to loop 7. With mutant Δ72–89, the black box represents the RRGGGGS sequence that replaced the $\beta$ hairpin (see the text). **B**: Location of the point mutations in the crystallographic structure of S7, adapted from Hosaka et al. (1997).

tered by the mutations, but does not exclude the possibility that minor perturbations could affect the tertiary folding of some mutants (data not shown). Comparison of the relative affinities in the high-ionic-strength and in the moderate-ionic-strength buffer emphasizes the importance of electrostatic interactions in the formation of the protein–RNA complex. Indeed, when the substitution of a charged residue influenced the binding of the protein, the effect was larger in the moderate-ionic-strength buffer (Fig. 5 and Table 2). Among the different mutations, the largest effects (a decrease of fivefold and more in the moderate-ionic-strength buffer)

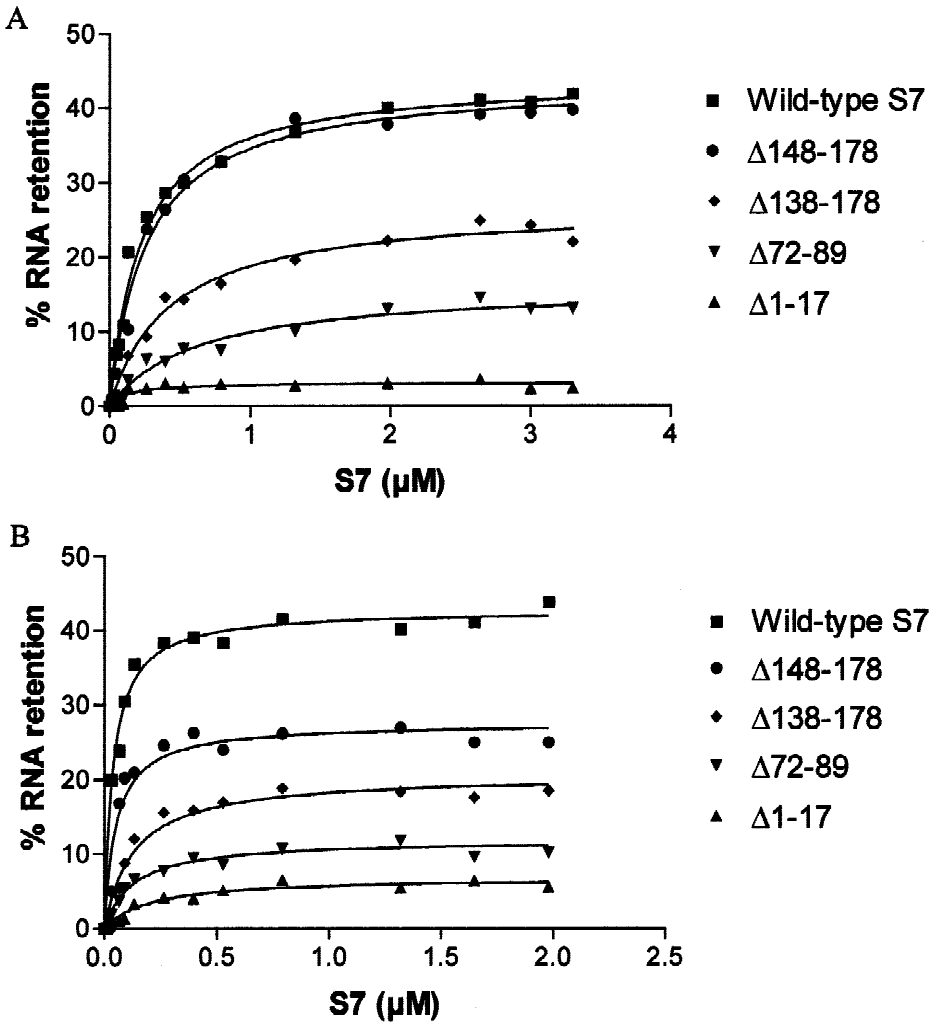


**FIGURE 4.** Binding curves for the interaction of wild-type S7 and its deletion derivatives with rRNA. The curves correspond to representative binding isotherms measured by a nitrocellulose filter binding assay. The lower half of the 3′ major domain of 16S rRNA was synthesized in vitro and incubated with increasing amounts of protein. Background retention of RNA on the filter (2–3% of the total rRNA) was subtracted before plotting. Binding constants are given in Table 1. **A**: Binding in a high-ionic-strength buffer. **B**: Binding in a moderate-ionic-strength buffer.

were obtained with Q8A and F17G in the N-terminal portion, with K35Q in loop 2, G54S in loop 3, and K113Q and M115G in loop 5. K34Q in loop 2 did not affect the binding in contrast to its neighbor K35Q. It was observed that the effect of the G54S mutation was increased in the moderate-ionic-strength buffer although this substitution does not directly involve a charged residue. Mutations in helix 6 (K136Q, R142Q, and M143A) also decreased the affinity but modestly. Y84A in the $\beta$ hairpin only decreased the affinity by about twofold, indicating that it does not play a major role in the interaction with the rRNA. The same observation holds for R3Q in the N-terminal region.

## DISCUSSION

Our results are in good agreement with the predictions made from the crystallographic structure of S7 (Hosaka et al., 1997; Wimberly et al., 1997). These predictions suggested that a large concave surface encompassing the $\beta$ hairpin and helices 4 and 6 plays an important role in the interactions between the protein and the rRNA. Our deletion mutation eliminating the $\beta$ hairpin severely reduces the affinity of S7 for the rRNA and supports the involvement of this region in rRNA binding. The effect of deleting helix 4 was not investigated because such a deletion would have perturbed the structure of the protein, but while our work was in progress, Miyamoto et al. (1999) published a report showing that point mutations in helix 4 as well as in the $\beta$ hairpin also decreased the interaction between *B. stearothermophilus* S7 and rRNA. Our results combined with those of Miyamoto et al. show that single point mutations in the $\beta$ hairpin and in helix 4 of S7 do not severely affect binding, suggesting that several weak contacts contribute to the interaction between the concave surface of

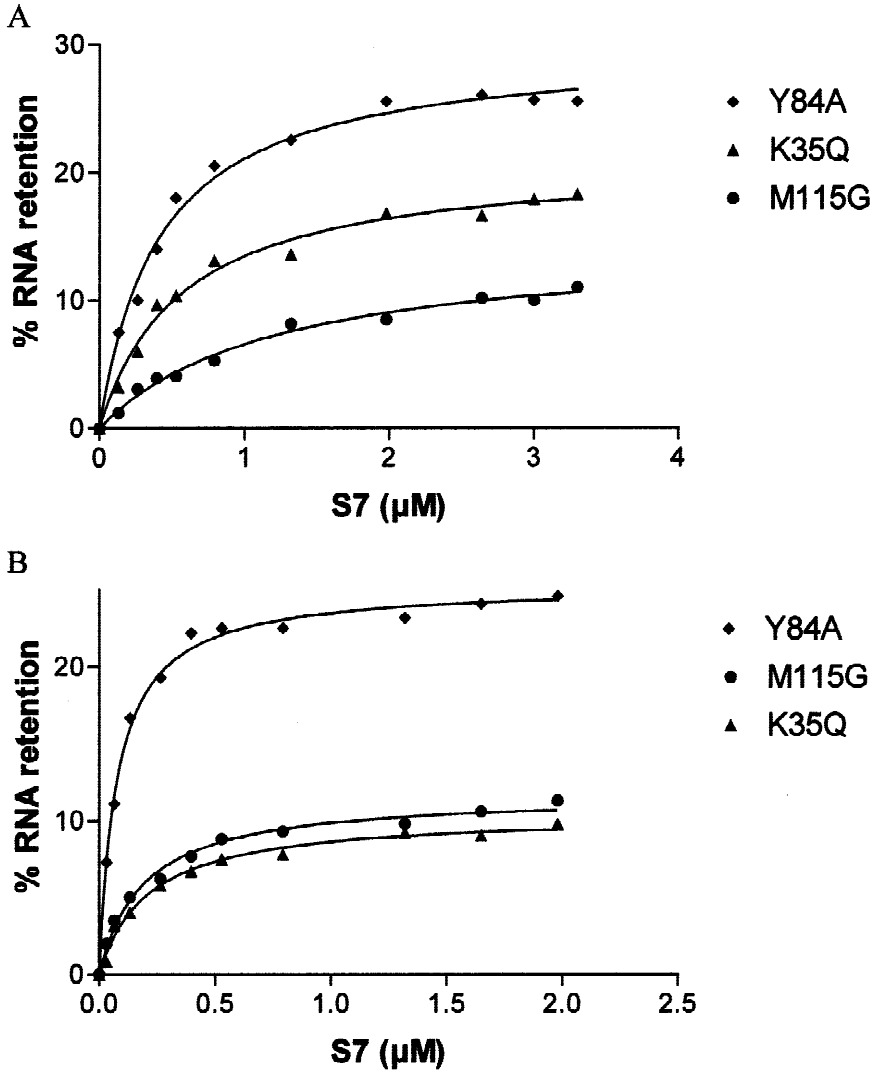


**FIGURE 5.** Binding curves for the interaction of S7 point mutants with rRNA. Typical binding curves are shown for a transcript corresponding to the lower half of the 3′ major domain of 16S rRNA. Conditions were as in Figure 4. Binding constants are given in Table 2. **A**: Binding in a high-ionic-strength buffer. **B**: Binding in a moderate-ionic-strength buffer.

protein S7 and the rRNA. This is shown, for instance, with mutation Y84A in our work and mutation R101Q in their work. Deleting a portion of helix 6 had a more modest effect than eliminating the $\beta$ hairpin. A modeling study by Tanaka et al. (1998) recently positioned the S7 crystallographic structure into a three-dimensional model of 16S rRNA. In their placement of the concave surface of S7, in agreement with the crosslink observed between K75 and nt 1378 of 16S rRNA (Urlaub et al., 1995, 1997) and with footprint sites for S7 (Powers et al., 1988; Powers & Noller, 1995), the $\beta$ hairpin interacts with the beginning of helix 29 and with loop B of 16S rRNA, and helix 4 of S7 runs along helix 29. Helix 6 of S7, which is proximal to the $\beta$ hairpin, could interact with the tip of helix 43 or, alternatively, it could contribute indirectly to S7 binding to the rRNA by interacting with the $\beta$ hairpin and influencing its orientation so as to optimize its contact with the rRNA.

Our results also stress the importance for rRNA binding of loops 2, 3, and 5, three loops that are well conserved and exposed to the solvent. Mutations in each of these loops strongly decreased the affinity of S7 for 16S rRNA. Loop 2, which connects helices 1 and 2, contains two positively charged K residues; whereas K34 substitution had no effect, K35 substitution severely impaired S7 binding, which can suggest a direct contact between this residue and rRNA, probably with the backbone. Loop 5 connects helices 4 and 5, and two substitutions within this loop, K113Q and M115G, severely impaired the binding of S7. A decreased binding when mutating loop 5 could be expected, because M115 was found to be crosslinked to U1240 at the junction between helices 30 and 41 of 16S rRNA (Urlaub et al., 1995, 1997). Loops 2 and 5 are neighbors in the crystal structure of S7, and the modeling of Tanaka et al. (1998) places them at the junction between

**TABLE 2.** Affinity for 16S rRNA of various point mutants of S7.

| Mutant | High ionic strength[a] | | Moderate ionic strength[b] | |
|---|---|---|---|---|
| | $K'_a$[c] ($\mu M^{-1}$) | Relative affinity | $K'_a$[c] ($\mu M^{-1}$) | Relative affinity |
| Wild-type S7 | 5.3 ± 0.5 | 1.00 | 30.5 ± 3.8 | 1.00 |
| R3Q | 3.0 ± 0.4 | 0.57 | 11.5 ± 1.6 | 0.38 |
| Q8A | 1.1 ± 0.2 | 0.21 | 7.9 ± 1.5 | 0.26 |
| F17G | 0.9 ± 0.2 | 0.17 | 6.4 ± 0.8 | 0.21 |
| K34Q | 5.5 ± 0.6 | 1.04 | 33.0 ± 5.3 | 1.08 |
| K35Q | 2.4 ± 0.5 | 0.45 | 4.2 ± 0.9 | 0.14 |
| G54S | 2.1 ± 0.4 | 0.40 | 4.9 ± 0.8 | 0.16 |
| Y84A | 3.4 ± 0.6 | 0.64 | 17.2 ± 2.8 | 0.56 |
| K113Q | 2.2 ± 0.3 | 0.42 | 7.3 ± 1.3 | 0.24 |
| M115G | 1.4 ± 0.3 | 0.26 | 7.8 ± 1.6 | 0.26 |
| K136Q | 5.2 ± 0.9 | 0.98 | 24.1 ± 3.5 | 0.79 |
| R142Q | 4.4 ± 0.9 | 0.83 | 20.1 ± 3.2 | 0.66 |
| M143A | 3.6 ± 0.7 | 0.68 | 11.8 ± 2.9 | 0.39 |

[a] High-ionic-strength buffer is 20 mM $MgCl_2$, 300 mM KCl.
[b] Moderate-ionic-strength buffer is 2 mM $MgCl_2$, 175 mM KCl.
[c] $K'_a$ values are means and standard deviation of at least four independent experiments.

helices 30 and 41 and near the beginning of helix 42, in agreement with the crosslinking data and the presence of several sites of protection of the RNA bases and backbone by S7 (Powers et al., 1988; Powers & Noller, 1995). Loop 3, which connects helices 2 and 3, is located on the face of S7, which is opposite to the concave surface and to loops 2 and 5. Mutation G54S in loop 3 severely decreased S7 binding. A previous report by Ehresmann et al. (1976) had shown that loop 3 could be UV-crosslinked to the 16S rRNA within the 30S subunit, suggesting that this loop directly interacts with the rRNA. The modeling of Tanaka et al. places it near an internal loop at the beginning of helix 41 of 16S rRNA, where protection occurs upon S7 binding. Neither the amino acid residue involved in loop 3 crosslink nor the site of crosslink on the rRNA were identified. An alternative suggestion is that loop 3 does not contact the rRNA and that this crosslink, which was not reported in subsequent studies, results from a transient interaction between the protein and the rRNA. The G54S mutation could indirectly affect S7 binding to the rRNA by introducing subtle rearrangements in the protein structure, which alter the orientation of helices and thus perturb some crucial contacts between the protein and the rRNA. These contacts probably involve electrostatic interactions, which could account for the greater effect of the G54S mutation in the moderate-ionic-strength buffer.

The N-terminal portion of S7 is rich in positively charged residues, a characteristic commonly found in the so-called arginine-rich motif that occurs in several RNA-binding proteins (Tan & Frankel, 1995). Deletion of the N-terminal 17 residues of S7 dramatically affected its affinity for rRNA because it caused a complete to near-complete loss of binding, depending upon the ionic strength of the binding buffer. A similar observation was made by Miyamoto et al. (1999) with the truncation of the N-terminal 10 residues of *B. stearothermophilus* S7. Point mutations within the N-terminal region also significantly affected S7 binding to rRNA, with a fivefold decrease of the affinity for mutants Q8A and F17G. The S7 terminal portion is an unstructured and flexible region, which has been crosslinked to C1378, the same base that was crosslinked to K75 in the $\beta$ hairpin (Urlaub et al., 1995, 1997; see Fig. 2) and is part of the P site (Green & Noller, 1997). It was also crosslinked to puromycin, an antibiotic that binds to the A site (Bischof et al., 1994). Moreover, directed hydroxyl radical probing showed that it is proximal to the loop capping helix 43 (Miyamoto et al., 1999). The results obtained with the mutations in the N-terminal portion indicate that this region of S7 plays a crucial role in the binding of the protein to rRNA, whereas the crosslinking studies and hydroxyl radical probing suggest that this region remains flexible when S7 is bound to rRNA. To account for the loss of binding in the absence of the N-terminal region, we propose that it makes an initial interaction with the rRNA that is required for the other contacts to occur. Once S7 is bound to the rRNA, the N-terminal region could disengage and then interact with the A site or with the P site. The flexibility of the N-terminal region of protein S7 makes it likely that the crosslinks involving this region and K75 can occur simultaneously within the 30S subunit. Alternatively, each of these crosslinks could correspond to a different conformational state of the 30S subunit. The N-terminal portion of S7 is not conserved in its eukaryotic homolog (Kuwano et al., 1992; Vladimirov et al., 1996; Wimberly et al., 1997), making this region an interesting potential target for the development of novel antibiotics that interfere with bacterial ribosome assembly. In various other RNA-binding ribosomal and nonribosomal proteins such as L1 (Eliseikina et al., 1996), the antitermination protein NusB of *E. coli* (Huenges et al., 1998), and the bacteriophage $\lambda$ N protein (Legault et al., 1998), the flexible and positively charged N-terminal portion has also been shown to play a crucial role in the interaction with the RNA.

When this work was completed, Fredrick et al. (2000) published a study that examined the effects of various mutations in *E. coli* S7 on 30S subunit assembly in vivo. The N-terminal deletion of S7 and mutations at positions 34 and 35 were also investigated by these researchers. Interestingly, the mutants with the N-terminal deletion or a substitution of K35, which bind weakly to the 16S rRNA in our experiments, are poorly incorporated into the 30S subunit in their assays, whereas the mutant with a substitution at position K34, which binds well to the rRNA, is efficiently incorporated into the 30S subunit. However, the good correlation between our results and those of Fredrick et al. does not hold for the mutant harboring a deletion of the $\beta$ hair-

pin, which is well-incorporated in their in vivo assays whereas its affinity for rRNA is weak in our in vitro assays. This suggests that the capacity of S7 to assemble into 30S subunits does not solely rely on its rRNA-binding activity.

The role of S7 in organizing the 3′ major domain of 16S rRNA warrants a detailed characterization of its interaction with 16S rRNA. X-ray crystallographic studies of the 30S subunit and the 70S ribosome are progressing at a very rapid pace and their structure will soon be available at an atomic resolution. It will, therefore, be important to investigate how these crystal structures explain the molecular basis of our mutagenesis results. It is, however, also possible that not all of the contacts used by S7 to bind to the naked rRNA and to initiate the assembly of the 30S subunit are maintained in the complete 30S particle.

## MATERIAL AND METHODS

### Chemicals and enzymes

All restriction endonucleases, alkaline phosphatase, and T4 DNA ligase were purchased from Amersham Pharmacia Biotech. Sequenase™ version 2.0 was from Amersham Life Sciences, and Deep Vent DNA polymerase was purchased from New England Biolabs. T7 RNA polymerase was purified from the overproducing strain BL21/pAR1219 as described (Zawadzki & Gross, 1991). [$\alpha$-$^{32}$P]-UTP (3,000 Ci/mmol) was from ICN. IPTG, PMSF, benzamidine, and lysozyme were purchased from Bioshop Canada Inc. All the oligonucleotides used were from GIBCO BRL.

### Plasmids and bacterial strains

Plasmid pET-21a(+), from Novagen, was used for the expression of protein S7 and its mutants under control of a T7 promoter. Competent *E. coli* XL1-Blue cells (Sambrook et al., 1989) were used for the transformation and storage of the various plasmids. *E. coli* BL21(DE3)/pLysS, which carries the T7 RNA polymerase gene under control of the *lacUV5* promoter, was used with pET-21a(+) and its derivatives for expression of protein S7 and its mutants (Studier et al., 1990).

### Cloning of the S7 gene and construction of S7 mutants

Genomic DNA from *E. coli* K12A19 was prepared by standard procedures (Marmur, 1961) and used for amplification of the S7 gene by PCR. The forward primer (#1) that contained a sequence coding for a histidine tag (italic letters) was: 5′-CGCGC**CATATG***CACCACCACCACCACCAC*CCAC GTCGTCGCGTCATTGGTC-3′, and the reverse primer (#2) was: 5′-GGCGC**CATATG**GGCGTTCAATTTAAGTAGCCC-3′. The underlined letters correspond to the initiation codon of S7 in primer #1 and the triplet complementary to the stop codon of S7 in primer #2. The bold letters in the primer sequences correspond to an *Nde*I restriction site that is used for the cloning of the PCR fragments containing the S7 gene or its mutants into pET-21a(+). PCR amplification of the S7 gene was carried out with the Deep Vent DNA polymerase in a Robocycler™ 40 from Stratagene under the following conditions: 5 min of denaturation at 94 °C, 25 cycles of 1 min at 94 °C, 1.5 min at the annealing temperature and 1 min at 72 °C, followed by a final extension step of 5 min at 72 °C. The amplified fragment was digested with *Nde*I, purified with the GFX™ PCR DNA and gel band purification kit (Amersham Pharmacia Biotech), and ligated into the appropriately digested plasmid pET-21a(+), generating pET-21a(+)-S7, which was subsequently used for the construction of the S7 mutants. The N-terminal deletion (Δ1–17) was created by PCR using a forward primer (#3) containing an *Nde*I site (bold letters) followed by the sequence for a histidine tag (italic letters), and designed such that the amplification of the S7 gene started at the codon corresponding to amino acid 18 (underlined letters): 5′-CGCGC**CATATG***CACCACCACCAC CACCAC*GGATCAGAACTGCTGGCTAAA-3′. Primer #2 was the reverse primer. The C-terminal deletions (Δ138–178 or Δ148–178) were also produced by PCR using the forward primer #1 and a reverse primer that introduced a stop codon (the underlined letters correspond to the triplet complementary to this codon) after residue 137 or 147 of S7: 5′-GGCGC**CATATG**ACGGTGAACGTCTCAACGTTTCTTAAC TGC-3′ (#4) and 5′-GGCGC**CATATG**GTGTGCGAACGA TTAGTTGGCTTCG-3′ (#5), respectively. The deletion of the $\beta$ hairpin (Δ72–89) was done by PCR in two steps. The first portion of the S7 gene (residues 1–71) was amplified with primer #1 as the forward primer, and the primer 5′-GGCCC**GGACC**CACCACCACCGCGGCGAGTCGGGCGCA CGTTTTCGAG-3′ (#6) as the reverse primer. The second portion of the gene (residues 90–178) was amplified with the forward primer 5′-GGCCCG**GGTCC**GTCCGTCCGGTTCGT CGTAATGCT-3′ (#7), and primer #2 as the reverse primer. The two PCR fragments were digested with *Ava*II (in bold letters for #6 and #7) and ligated together. Primers #6 and #7 were designed such that a sequence coding for RRGGGGS was added at the junction of the two PCR fragments, replacing the $\beta$ hairpin sequence (residues 72–89) with a short loop of seven residues. This avoids a drastic structural perturbation by recreating the charged environment of this region of the protein. PCR conditions for the deletion mutants were as described above.

The plasmids coding for the substitution mutants of S7 were derived from pET-21a(+)-S7 by a two-step PCR, using the overlap extension procedure described by Ho et al. (1989). The flanking primers, 5′-TAATACGACTCACTATAGGGG-3′ (#8) and 5′-TAGTTATTGCTCAGCGGTGGC-3′ (#9), annealed to the T7 promoter region and to the T7 terminator region, respectively, on the pET plasmid. The internal mutagenic primers used to introduce the mutations were entirely overlapping and, for each mutation, only one of the complementary primers with the same orientation as primer #8 is indicated here: R3Q: 5′-CCACCCACGTCAGCGCGTCATTG-3′ (#10); Q8A: 5′CGTCATTGGTGCGCGTAAAATTC-3′ (#11); F17G: 5′-GG ATCCGAAGGGCGGATCAGAAC-3′ (#12); K34Q: 5′-GGTA GATGGTCAGAAATCTACTG-3′ (#13); K35Q: 5′-AGATGGT AAACAGTCTACTGCTG-3′ (#14); G54S: 5′-TCAGCGCTCT AGCAAATCTGAAC-3′ (#15); Y84A: 5′-TGGTTCTACTGCG CAGGTACCAG-3′ (#16); K113Q: 5′-ACGCGGTGATCAG TCCATGGCTC-3′ (#17); M115G: 5′-TGATAAATCCGGCGC TCTGCGCC-3′ (#18); K136Q: 5′-TGCAGTTAAGCAGCGTG AAGACG-3′ (#19); K142Q: 5′-AGACGTTCACCAGATGGC

CGAAG-3′ (#20); M143A; 5′-CGTTCACCGTGCGGCCGAA GCCA-3′ (#21). The underlined letters correspond to the mutated codon. The coding sequence of S7 and all its mutant derivatives were verified by the dideoxynucleotide sequencing method (Sanger et al., 1977).

### Expression and purification of S7 and its derivatives

S7 and its derivatives were expressed in *E. coli* BL21(DE3)/pLysS as described by Studier et al. (1990). Expression was induced for 3 h with 1 mM IPTG at 37 °C when the culture reached an $OD_{600}$ of about 0.6. Cells were harvested and sonicated and the proteins were purified by chromatography under native conditions on a Ni-NTA resin (Novagen) as described by the manufacturer. The purity of the proteins was assessed by SDS-PAGE and their concentration was determined by a Bradford assay (BioRad). The fractions containing the proteins were pooled and dialyzed against a high-ionic-strength buffer, HMK (50 mM HEPES-KOH, pH 7.8, 20 mM $MgCl_2$, 300 mM KCl, and 5 mM $\beta$-mercaptoethanol), containing 0.01% Triton X-100. Aliquots of the protein solutions were conserved at −80 °C.

### Synthesis of the lower half of the 3′ major domain of 16S rRNA

Synthesis of the [$^{32}$]P-labeled 16S rRNA fragment that binds S7 was carried out by in vitro transcription with T7 polymerase of plasmid pFD3LH (Dragon & Brakier-Gingras, 1993). This plasmid contains the rDNA sequence corresponding to the lower half of the 3′ major domain plus the 3′ minor domain of 16S rRNA (nt 926-986/1219–1542). It was linearized with *Rsa*I and transcribed as described by Dragon & Brakier-Gingras (1993), generating the lower half of the 3′ major domain (nt 926–986/1219–1393).

### Filter binding assays

The interaction between the various S7 mutants and the 16S rRNA fragment was assessed by the nitrocellulose filter binding assay, as described by Dragon & Brakier-Gingras (1993), with minor modifications. The RNA fragment was incubated at 43 °C for 30 min in the binding buffer, the protein was then added at various concentrations, and the mixture was left for 30 min at 30 °C, and kept on ice for at least 10 min prior to filtration. The binding buffer was either the high-ionic-strength (HMK) buffer or a moderate-ionic-strength buffer, where $MgCl_2$ was 2 mM and KCl was 175 mM. The $K'_a$ was calculated using GraphPad Prism version 3.00 for Windows, GraphPad Software, San Diego, California, USA; www.graphpad.com.

### Circular dichroism

Circular dichroism spectra were recorded at 4 °C on a Jasco J-710 spectropolarimeter, using a cylindrical cuvette with a 0.1-cm path length. Spectra were taken between 190 and 260 nm in HMK buffer at protein concentrations ranging from 0.2 to 0.4 mg/mL. Because of the high chloride concentration in the buffer, the spectra were not reliable below 210 nm.

## ACKNOWLEDGMENTS

We thank M. Aubry, G. Boileau, F. Dragon, and R. Zimmermann for helpful discussions and comments. This work was supported by a grant from the Medical Research Council of Canada to L.B.-G.

*Received June 29, 2000; returned for revision July 20, 2000; revised manuscript received July 26, 2000*

## REFERENCES

Alexander RW, Muralikrishna P, Cooperman BS. 1994. Ribosomal components neighboring the conserved 518–533 loop of 16S rRNA in 30S subunits. *Biochemistry 33*:12109–12118.

Bischof O, Kruft V, Wittmann-Liebold B. 1994. Analysis of the puromycin binding site in the 70S ribosome of *Escherichia coli* at the peptide level. *J Biol Chem 269*:18315–18319.

Brimacombe R. 1991. RNA–protein interactions in the *Escherichia coli* ribosome. *Biochimie 73*:927–936.

Buck MA, Cooperman BS. 1990. Single protein omission reconstitution studies of tetracycline binding to the 30S subunit of *Escherichia coli* ribosomes. *Biochemistry 29*:5374–5379.

Capel MS, Engelman DM, Freeborn BR, Kjeldgaard M, Langer JA, Ramakrishnan V, Schindler DG, Schneider DK, Schoenborn, BP, Sillers IY, Yabuki S, Moore PB. 1987. A complete mapping of the proteins in the small ribosomal subunit of *Escherichia coli*. *Science 238*:1403–1406.

Cate JH, Yusupov MM, Yusupova GZ, Earnest TN, Noller HF. 1999. X-ray crystal structures of 70S ribosome functional complexes. *Science 285*:2095–2104.

Clemons WM Jr, May JL, Wimberly BT, McCutcheon JP, Capel MS, Ramakrishnan V. 1999. Structure of a bacterial 30S ribosomal subunit at 5.5 Å resolution. *Nature 400*:833–840.

Dijk J, Littlechild JA, Freund AM, Pouyet J, Daune M, Provencher SW. 1986. The secondary structure of salt-extracted ribosomal proteins from *Escherichia coli* as studied by circular dichroic spectroscopy. *Biochim Biophys Acta 874*:227–234.

Dontsova O, Dokudovskaya S, Kopylov A, Bogdanov A, Rinke-Appel J, Jünke N, Brimacombe R. 1992. Three widely separated positions in the 16S RNA lie in or close to the ribosomal decoding region: A site-directed cross-linking study with mRNA analogues. *EMBO J 11*:3105–3116.

Döring T, Mitchell P, Osswald M, Bochkariov D, Brimacombe R. 1994. The decoding region of 16S RNA: A cross-linking study of the ribosomal A, P and E sites using tRNA derivatized at position 32 in the anticodon loop. *EMBO J 13*:2677–2685.

Dragon F, Brakier-Gingras L. 1993. Interaction of *Escherichia coli* ribosomal protein S7 with 16S rRNA. *Nucleic Acids Res 21*:1199–1203.

Dragon F, Payant C, Brakier-Gingras L. 1994. Mutational and structural analysis of the RNA binding site for *Escherichia coli* ribosomal protein S7. *J Mol Biol 244*:74–85.

Draper DE. 1999. Themes in RNA–protein recognition. *J Mol Biol 293*:255–270.

Ehresmann B, Reinbolt J, Backendorf C, Tritsch D, Ebel JP. 1976. Studies of the binding sites of *Escherichia coli* ribosomal protein S7 with 16S RNA by ultraviolet irradiation. *FEBS Lett 67*:316–319.

Eliseikina IA, Avliyakulov NK, Grishkovskaya IB, Muranova TA, Sedelnikova SE, Garber MB. 1996. RNA binding properties of ribosomal protein L1 from *Thermus thermophilus. Biochemistry (Moscow) 61*:1461–1464.

Fredrick K, Dunny GM, Noller HF. 2000. Tagging ribosomal protein S7 allows rapid identification of mutants defective in assembly and function of 30S subunits. *J Mol Biol 298*:379–394.

Green R, Noller HF. 1997. Ribosomes and translation. *Annu Rev Biochem 66*:679–716.

Gregory RJ, Cahill PBF, Thurlow DL, Zimmermann RA. 1988. Interaction of *Escherichia coli* ribosomal protein S8 with its binding sites in ribosomal RNA and messenger RNA. *J Mol Biol 204*:295–307.

Greuer B, Thiede B, Brimacombe R. 1999. The cross-link from the

upstream region of mRNA to ribosomal protein S7 is located in the C-terminal peptide: Experimental verification of a prediction from modeling studies. *RNA 5*:1521–1525.

Gutell RR, Larsen N, Woese CR 1994. Lessons from an evolving rRNA: 16S and 23S rRNA structures from a comparative perspective. *Microbiol Rev 58*:10–26.

Ho SN, Hunt HD, Horton RM, Pullen JK, Pease LR. 1989. Site-directed mutagenesis by overlap extension using the polymerase chain reaction. *Gene 77*:51–59.

Hosaka H, Nakagawa A, Tanaka I, Harada N, Sano K, Kimura M, Yao M, Wakatsuki S. 1997. Ribosomal protein S7: A new RNA-binding motif with structural similarities to a DNA architectural factor. *Structure 5*:1199–1208.

Huenges M, Rölz C, Gschwind R, Peteranderl R, Berglechner F, Richter G, Bacher A, Kessler H, Gemmecker G. 1998. Solution structure of the antitermination protein NusB of *Escherichia coli*: A novel all-helical fold for an RNA-binding protein. *EMBO J 17*:4092–4100.

Johanson U, Hughes D. 1992. Comparison of the complete sequence of *str* operon in *Salmonella typhimurium* and *Escherichia coli. Gene 120*:93–98.

Kao-Huang Y, Revzin A, Butler AP, O'Conner P, Noble DW, von Hippel PH. 1977. Nonspecific DNA binding of genome-regulating proteins as a biological control mechanism: Measurement of DNA-bound *Escherichia coli lac* repressor *in vivo*. *Proc Natl Acad Sci USA 74*:4228–4232.

Karginov AV, Karginova OA, Spiridonova VA, Kopylov AM. 1995. In vivo assembly of plasmid-expressed ribosomal protein S7 of *Thermus thermophilus* into *Escherichia coli* ribosomes and conditions of its overexpression. *FEBS Lett 369*:158–160.

Kuwano Y, Olvera J, Wool IG. 1992. The primary structure of rat ribosomal protein S5: A ribosomal protein present in the rat genome in a single copy. *J Biol Chem 267*:25304–25308.

Legault P, Li J, Mogridge J, Kay LE, Greenblatt J. 1998. NMR structure of the bacteriophage $\lambda$ N peptide/*boxB* RNA complex: Recognition of a GNRA fold by an arginine-rich motif. *Cell 93*: 289–299.

Marmur J. 1961. A procedure for the isolation of deoxyribonucleic acid from microorganisms. *J Mol Biol 3*:208–218.

Miyamoto A, Usui M, Yamasaki N, Yamada N, Kuwano E, Tanaka I, Kimura, M. 1999. Role of the N-terminal region of ribosomal protein S7 in its interaction with 16S rRNA which binds to the concavity formed by the $\beta$-ribbon arm and the $\alpha$-helix. *Eur J Biochem 266*:591–598.

Mueller F, Brimacombe R. 1997. A new model for the three-dimensional folding of *Escherichia coli* 16S ribosomal RNA. II. The RNA–protein interaction data. *J Mol Biol 271*:545–565.

Muralikrishna P, Cooperman BS. 1994. A photolabile oligodeoxyribonucleotide probe of the decoding site in the small subunit of the *Escherichia coli* ribosome: Identification of neighboring ribosomal components. *Biochemistry 33*:1392–1398.

Nowotny V, Nierhaus KH. 1988. Assembly of the 30S subunit from *Escherichia coli* ribosomes occurs via two assembly domains which are initiated by S4 and S7. *Biochemistry 27*:7051–7055.

Powers T, Noller HF. 1995. Hydroxyl radical footprinting of ribosomal proteins on 16S rRNA. *RNA 1*:194–209.

Powers T, Changchien LM, Craven GR, Noller HF. 1988. Probing the assembly of the 3′ major domain of 16S ribosomal RNA. Quaternary interactions involving ribosomal proteins S7, S9 and S19. *J Mol Biol 200*:309–319.

Reinbolt J, Tritsch D, Wittmann-Liebold B. 1978. The primary structure of ribosomal protein S7 from *E. coli* strains K and B. *FEBS Lett 91*:297–301.

Rosen KV, Zimmermann RA. 1997. Photoaffinity labeling of 30S-subunit proteins S7 and S11 by 4-thiouridine-substituted $tRNA^{Phe}$ situated at the P site of *Escherichia coli* ribosomes. *RNA 3*:1028–1036.

Saito K, Mattheakis LC, Nomura M. 1994. Post-transcriptional regulation of the *str* operon in *Escherichia coli.* Ribosomal protein S7 inhibits coupled translation of S7 but not its independent translation. *J Mol Biol 235*:111–124.

Saito K, Nomura M. 1994. Post-transcriptional regulation of the *str* operon in *Escherichia coli.* Structural and mutational analysis of the target site for translational repressor S7. *J Mol Biol 235*:125–139.

Sambrook J, Fritsch EF, Maniatis T. 1989. *Molecular cloning: A laboratory manual.* Cold Spring Harbor, New York: Cold Spring Harbor Laboratory Press. p 59.

Sanger F, Nicklen S, Coulson AR. 1977. DNA sequencing with chain-terminating inhibitors. *Proc Natl Acad Sci USA 74*:5463–5467.

Spiridonova VA, Golovin AV, Drygin DY, Kopylov AM. 1998. An extremely high conservation of RNA-protein S7 interactions during prokaryotic ribosomal biogenesis. *Biochem Mol Biol Int 44*:1141–1146.

Studier FW, Rosenberg AH, Dunn JJ, Dubendorff JW. 1990. Use of T7 RNA polymerase to direct expression of cloned genes. *Methods Enzymol 185*:60–89.

Sylvers LA, Kopylov AM, Wower J, Hixon SS, Zimmermann RA. 1992. Photochemical cross-linking of the anticodon loop of yeast $tRNA^{Phe}$ to 30S-subunit protein S7 at the ribosomal A and P sites. *Biochimie 74*:381–389.

Tan R, Frankel AD. 1995. Structural variety of arginine-rich RNA-binding peptides. *Proc Natl Acad Sci USA 92*:5282–5286.

Tanaka I, Nakagawa A, Hosaka H, Wakatsuki S, Mueller F, Brimacombe R. 1998. Matching the crystallographic structure of ribosomal protein S7 to a three-dimensional model of the 16S ribosomal RNA. *RNA 4*:542–550.

Tocilj A, Schlünzen F, Janell D, Glühmann M, Hansen HAS, Harms J, Bashan A, Bartels H, Agmon I, Franceschi F, Yonath A. 1999. The small ribosomal subunit from *Thermus thermophilus* at 4.5 Å resolution: Pattern fittings and the identification of a functional site. *Proc Natl Acad Sci USA 96*:14252–14257.

Urlaub H, Kruft V, Bischof O, Müller EC, Wittmann-Liebold B. 1995. Protein–rRNA binding features and their structural and functional implications in ribosomes determined by cross-linking studies. *EMBO J 14*:4578–4588.

Urlaub H, Thiede B, Müller EC, Brimacombe R, Wittmann-Liebold B. 1997. Identification and sequence analysis of contact sites between ribosomal proteins and rRNA in *Escherichia coli* 30S subunits by a new approach using matrix-assisted laser desorption/ionization-mass spectroscopy combined with N-terminal microsequencing. *J Biol Chem 272*:14547–14555.

Vladimirov SN, Ivanov AV, Karpova GG, Musolyamov AK, Egorov TA, Thiebe B, Wittmann-Liebold B, Otto A. 1996. Characterization of the human small-ribosomal-subunit proteins by N-terminal and internal sequencing, and mass spectrometry. *Eur J Biochem 239*:144–149.

Wimberly BT, White SW, Ramakrishnan V. 1997. The structure of ribosomal protein S7 at 1.9 Å resolution reveals a $\beta$-hairpin motif that binds double-stranded nucleic acids. *Structure 5*:1187–1198.

Zawadzki V, Gross HJ. 1991. Rapid and simple purification of T7 RNA polymerase. *Nucleic Acids Res 19*:1948.